Journal of Physics:
Conference Series

PAPER • OPEN ACCESS

Biaxial loading after low-velocity impact response on scarf repair glass fibre reinforced polymer (GFRP)

To cite this article: Menatalla M. Ismail *et al* 2025 *J. Phys.: Conf. Ser.* **3070** 012013

Biaxial loading after low-velocity impact response on scarf repair glass fibre reinforced polymer (GFRP)

Menatalla M. Ismail[1]*, Mostafa Shazly[1], Mohamed M. El-Sayed Seleman[2] and George S. A. Fam[1]

[1] Mechanical Engineering Department, The British University in Egypt, Cairo, Egypt.,
[2] Department of Metallurgical and Materials Engineering, Faculty of Petroleum and Mining Engineering, Suez University, Suez 43512, Egypt.,

*E-mail: Menatalla.ismail@bue.edu.eg

Abstract. The composite material has become one of the most used materials in several applications, such as aviation, marine, and civil sectors, because of its lightweight and high-strength properties. Therefore, the wide use of this material has made it essential to explore its durability and efficiency, in particular, after repair processes. The present work investigates the effect of impact energy and its location on the remaining strength of scarf-repaired glass fibre composite. The study was conducted in two phases; in the first phase, a low-velocity impact test was carried out at specified impact locations according to the central composite statistical experimental model. A visual inspection was then performed to evaluate the damage size to the impact energy. In the second phase, tests based on biaxial loading were performed up to the failure of the repair. Then, a central composite design model was used to explore the effect of various factor levels. Results showed that the model fits firmly by 93.07% of the variability in biaxial loading. Additionally, the model showed that both factors were significant and correlated negatively with the response; however, the impact location was more sensitive than the impact energy. The critical locations were found to be around the edge of the repair.

1. Introduction

One of the leading causes of climate change is the greenhouse emissions caused by several industries. The emissions produced by any fuel combustion sector are comparable as they all include carbon dioxide, nitrogen oxides, and sulfuric oxides. Emissions from aircraft engines are released directly into the upper troposphere, making this one of the significant environmental effects compared to other factors causing ground-level emissions. Over the past 50 years, the aviation industry has gained considerable attention regarding noise, air pollution, and climate change.[1], [2] As a result, composite materials have revolutionised the aviation industry due to their various advantages over traditional materials. Lightweight and high specific strength composite materials have resulted in improved fuel efficiency. Their mechanical and chemical properties ensure durability under several conditions and resistance to corrosion. In addition, adopting composite materials has improved sustainability and aligned the aviation industry with carbon reduction by 14-15% as the target, making them environmentally friendly. As a result, the study of composite repair is essential for ensuring safety and integrity since efficient repair techniques can prevent critical failures and reduce maintenance costs [3,4]. However, besides composite materials' notable properties, they are always susceptible to impact loads from several causes, such as tool drops, bird strikes, and accidental impacts such as hard landings. These damages include fibre failure, matrix cracking, or delamination. These failures downgrade the mechanical properties and, therefore, decrease the lifetime. Repair is then required to restore the lost strength [5,6]. Research in this area has also increased the lifetime of composite components and failure responses to different damage mechanisms to meet the aviation industry standards and highlight the importance of continuing research in this field [3].

Composite laminate repair has been performed using various techniques, including adhesive bonding, mechanical fastening, or combining both methods [7]. When comparing these techniques, adhesive bonding repair has many advantages over mechanical fasteners. These include weight reduction by eliminating fasteners, uniform load distribution, and maintaining aerodynamic smoothness. When the adhesive repair decreases the stress concentration, fatigue and delamination failure risk are enhanced. In addition, sealing protection has been offered against corrosion and moisture. Finally, adhesive bonded repair is preferred in most composite applications due to its durability, efficiency, and strength. On the other hand, mechanical fastener repair is certified and standardised due to easier inspection. In contrast, the inspection of adhesive repair is challenging, calling for further research and studies [8].

Bonded composite repairs are divided into several types based on the application. Scarf repair involves removing the damaged area in thick sections to create a smooth taper bond surface to distribute the stresses. Patch repair uses composite patches over the damaged areas. Stepped scarf/lap repair uses stepped layered laminates to improve the strength. Doubler repair adds a layer over the damaged area to enhance strength, while lap repair adds more than one layer to be bonded over the damaged area. The last type is composite laminate repair, which involves bonding layers in different configurations. Each type has advantages and disadvantages and can be tailored depending on the damage condition and the application [9].

According to previous research, scarf repair is one of the preferred repairs compared to other techniques. Bendemra et al. [10] found that the scarf joint is efficient in stress distribution compared to the stepped lap joint. This also aligned with Odi and Friend's [11] conclusion that scarf repair has better stress concentration, load transfer, and high adhesive strength when compared to stepped lap repair. Similarly, Srinivasan et al. [12] has compared scarf repair with strapped joints, finding a similar conclusion. Finally, Barbosa et al. [13] has compared the most common four adhesive bonded configurations to find that the scarf repair has better stress distribution compared to single and double lap joints and better strength when compared to single lap and stepped joints.

Much research has been conducted on different loadings, such as tensile and compression, after the low-velocity impact of intact laminates. However, few studies have tested low-velocity impact on repaired composite structures [14,15] or with different ranges of impact energies. Few studies have used constant mass with various heights to vary the impact energy on scarf repair samples. It is essential to know that studying low-velocity impact on scarf repair is critical since it generates several types of damage to the composites, such as delamination, matrix cracks or fibre breakage. Most of these damages are internal and hard to detect. For example, damages such as barely visible impact damage (BVID) are impacts on a small scale and are difficult to locate but can lead to catastrophic failure [16].

Shankar and Idapalapati [17] have studied the impact resistance of different geometrical scarf-repaired specimens and found that the circular shape exhibits superior impact resistance and minimises damage compared to other geometries. Deng et al. [18] have studied the bonding defects in scarf-repaired composites when exposed to tensile tests. They found that bonding defects weaken the repaired area and lower the load capacity. Moreover, it has also been found that the patch's stacking sequence and rotation angle also affect the low-velocity impact performance [19]. Kumari et al. [20] have tested tensile after low-velocity impact in four different locations on scarf repair and two different energy levels to conclude that impact response varies with impact location using both energy levels. They also noted that the impact at the bond line shows the least tensile loading, while the impact outside the repaired region is not critical. The same authors [21] studied the effect of multiple impacts on composite scarf-repaired specimens using tensile tests. They observed that each repeated impact results in more damage. According to the post-tensile response analysis, the composite samples with the highest ultimate load in the post-tensile test were those that had the least amount of energy absorption or dent damage during the impact test.

While Response Surface Methodology offers multiple models [22], the Central Composite Design (CCD) is recognized as a particularly effective experimental design. CCD is a well-organised and efficient composition model since it requires reduced experimental trials and can depict complex responses. With few tests, CCD enables researchers to optimise processes, find non-linear effects, and analyse various factor values. This makes it a practical instrument for conducting informative and economical experiments across multiple industries.

This research aims to investigate the impact response on scarf-repaired specimens with various energy levels and impact locations using the CCD statistical model. Moreover, the Biaxial loading is carried out to examine the residual strength of the glass fibre-reinforced polymer after repair and impact. Biaxial loading has been chosen rather than tensile, following the literature review, because it simulates general loading cases experienced by the material.

2. Theoretical Model

2.1 Specimens Fabrication

A GFRP panel having a total of 7 laminas of glass fibre, each has three plies (-45°/90°/45°) with an areal density of 900 gm/m^2 was fabricated using the hand lamination technique on a glass plate. The resin used is a two-component epoxy, Araldite LY 1564 SP (Bisphenol-A Epoxy Resin from Huntsman) and its hardener Aradur 3486 CH (Polyamine Epoxy Hardener from Huntsman) with a ratio of (3:1). During the fabrication process, the glass plate was first cleaned with a thinner to remove any dust, and then a sufficient and uniform wax layer was applied. The seven laminates were placed one after the other while the resin was applied thoroughly using a painting roll. Finally, another glass plate is waxed and placed over the laminates with applied loads to remove excess resin and any bubbles. After this, the fabricated plate was left for 4 days under pressure at room temperature for full curing. After curing, the composite plate was removed from the mould and cut into 15 specimens with square shapes of 150mm × 150mm × 5mm using a water-cooled wafering saw, as shown in Figure 1.

2.2 Repair technique

A circular hole with a radius of 5 mm and a scarf angle of 10 was machined using a CNC milling machine in the cut specimens. The hole was polished using sandpaper, and the area was cleaned to remove any residuals. All the samples were prepared with similar thicknesses and designs.

According to ASTM D2093-03, each scarfed sample was prepared through identical scarfing steps. Seven layers of plies were cut into circular shapes using a laser machine to ensure the accuracy of small diameters, as shown in Figure 2. These diameters were calculated using the scarf angle and the geometry of the taper hole. Furthermore, the same resin was applied over the tapered hole, and the plies rolled by the resin one after the other. The pressure was applied to the scarf hole to ensure that the resin and plies entirely covered the scarf hole to avoid void formation. The curing process was also done at room temperature.

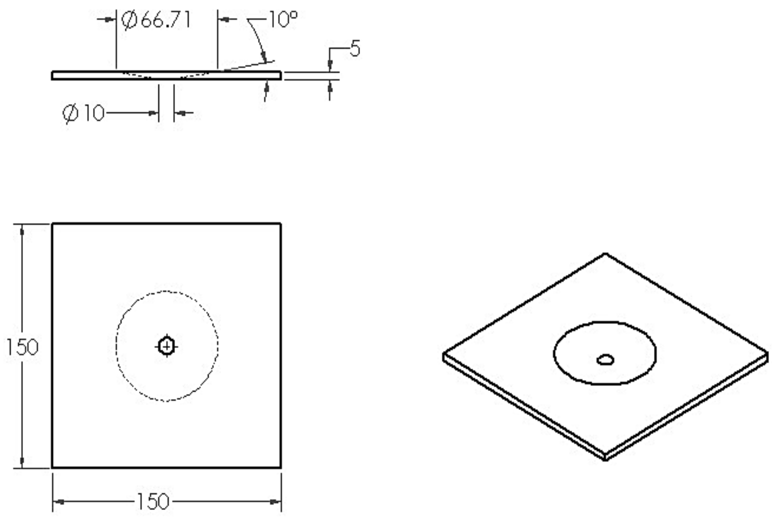

Figure 1. Scarfed composite laminate design and dimensions

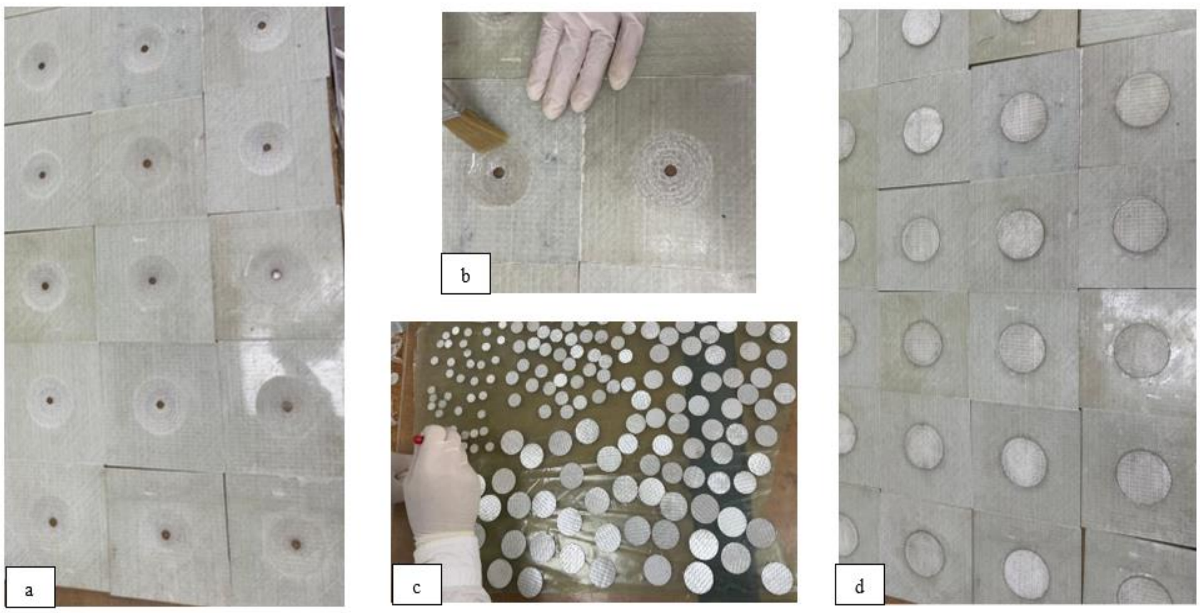

Figure 2. a) specimens after sanding, b) Resin applied, c) plies rolled with resin, d) final specimens before applying biaxial loading

2.3 Statistical analysis

The central composite design (CCD) was adopted in the present work. CCD is a design of an experiment model that captures the maximum amount of data by using a small number of specimens. Furthermore, it captures any nonlinearity between the factors and the output. Due to its widespread use, the Spherical Central Composite Design (SCCD) was chosen as the model, and Table 1. displays the resulting experimental data ranges.

Table 1. Central composite design statistics

Factor	Description
A	Energy
Units	J
Type	Numerical
Minimum	6.8
Maximum	28.1
Coded Low	-1 ↔ 10.00
Coded High	+1 ↔ 25.00
B	Location
Units	mm
Type	Numerical
Minimum	-6.6
Maximum	38
Coded Low	-1 ↔ 0.00
Coded High	+1 ↔ 32.00

2.4 Impact test

After the repair process, the specimens were marked with the exact impact locations. Impact energies, ranging from 6 to 28 J, were generated by altering the drop height. The resulting energy values were then calculated using Equation 1., considering the mass of the spherical indenter.

$$\boldsymbol{E = m\,g\,H} \tag{1}$$

Where E is impact energy (J), H is impact height (m), m is the mass of the impact ball (kg), and g is gravitational acceleration (9.8 m/s^2).

The impact test was performed using the Drop Tower according to ASTM D7136/D7136M–12, as shown in Figure 3. First, the specimen is fixed, and the impact location is adjusted. The height needed for the specified energy is also adjusted before the weight is freely dropped to the specified locations shown in Figure 4. Following the impact tests, all specimens were examined visually to assess the damage.

2.5 Biaxial loading test

Impacted specimens were visually inspected and photographed to analyse the damage under various energy levels. The impacted specimens were then tested under biaxial loading using the setup shown in Figure 5. This setup consists of a circular clamping cover over an oil reservoir where the specimen is fixed using 8 screws to avoid any oil leakage. Under this clamping cover, an oil pump supplies the pressure to the reservoir. The oil pressure is increased incrementally until the specimen fails and the oil leaks. Failure pressure was determined by recording the peak pressure from the pressure gauge.

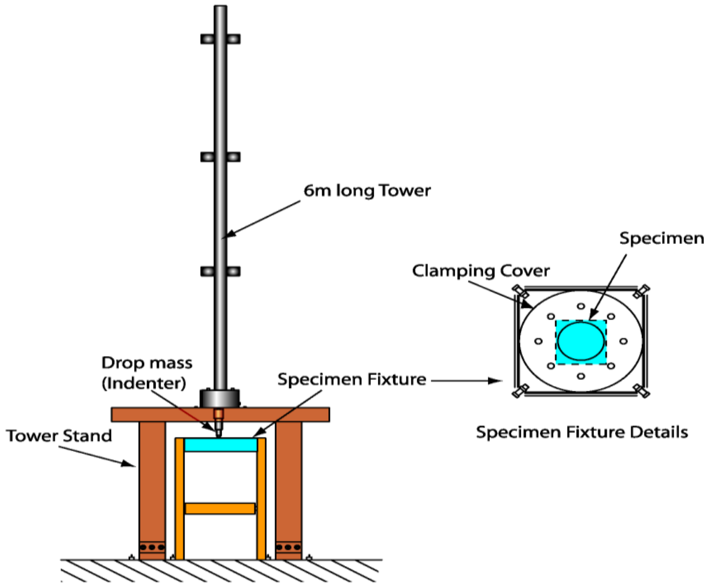

Figure 3. Drop Tower Impact Test Set-up

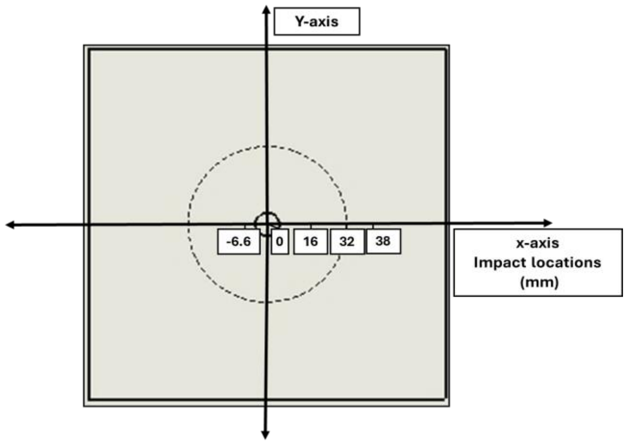

Figure 4. Impact locations marked for testing

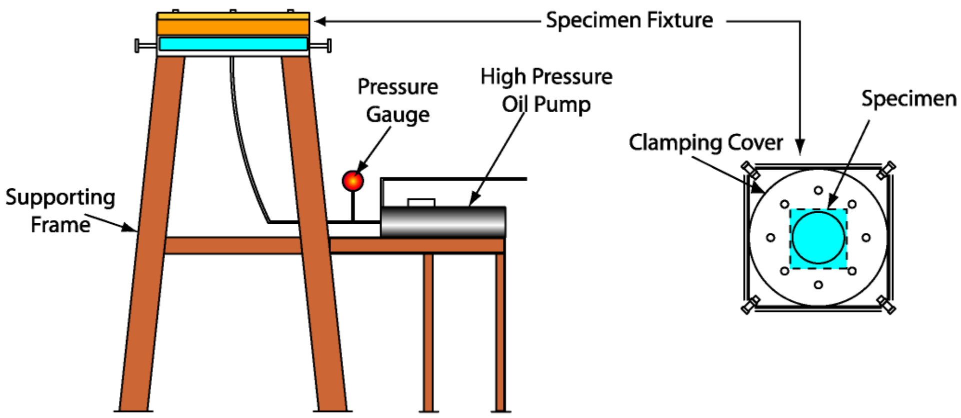

Figure 5. Biaxial loading Set-up.

3. Results and Discussion

3.1 Impact Damage Visual Inspection

A visual inspection was conducted on the tested specimens to identify any apparent differences after the impact was generated at different energy levels and locations. Based on the literature, when impact energy increases, the damaged area also increases. Figure 6. shows the dimensions of the damaged areas as measured by ImageJ software on the impacted specimens.

3.2 Statistical Analysis Results

Table 2**.** shows the experimental results obtained during the impact test and subsequent biaxial loading. This data was used in a Statistical code in MATLAB to study the tendency of the experimental results. First, the experimental design and model were studied by indicating the statistical metrics, as shown in Table 3. R-squared suggests that this model explains 93.07% of the variation in this experiment, and the adjusted R-squared is 88.12%, indicating that the model provides a good explanation and prediction even after facing any predictors. Secondly, the F and P values show that the model is highly significant and effective.

Additionally, the ANOVA table was extracted to estimate the effect of each factor in the model and their significance, as shown in Table 4. First was impact energy, indicating that the Biaxial loading (response) variable decreases by 0.9264 units for each unit increase, showing a clear inverse relation between impact energy and the biaxial loading. Also, the P value of the impact energy was less than 0.05, which confirms that this factor is statistically significant. Secondly was the impact location, which also had a negative coefficient with the response but with a higher value than impact energy and a much lower P value, indicating that the impact location strongly affects the response when comparing it to the impact energy. Thirdly, the interaction between the two factors was insignificant since the P value was more significant than 0.05. It was also not a high value, which might indicate that a small interaction effect could become important with a larger sample size in the future.

Table 2. Composite performance in biaxial loading after impact

Run Order& Specimen No.	Impact energy (J)	Impact location (mm)	Biaxial loading Failure pressure (bar)
1	10	0	11.9
2	25	0	10
3	10	32	8
4	25	32	7.5
5	17.5	16	10
6	17.5	16	9.8
7	17.5	16	10
8	17.5	16	10
9	17.5	16	10
10	28.11	16	9.5
11	6.89	16	11.5
12	17.5	38	8
13	17.5	-6.6	11

Journal of Physics: Conference Series **3070** (2025) 012013 doi:10.1088/1742-6596/3070/1/012013

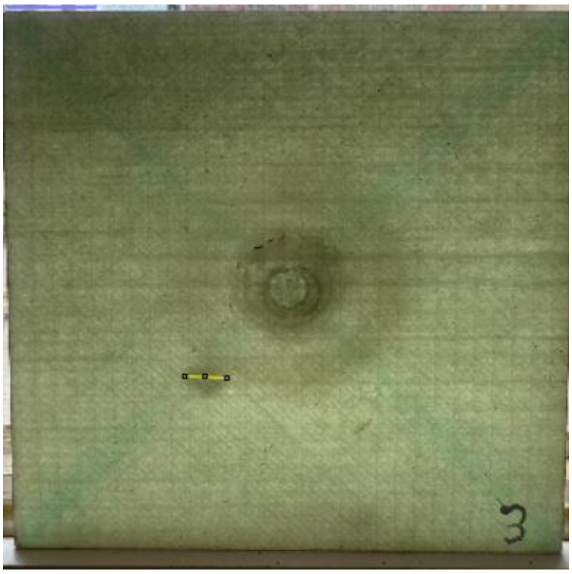

Specimen 3
Impact energy = 10 J
Impact location =32 mm
Damage length= 11.2 mm

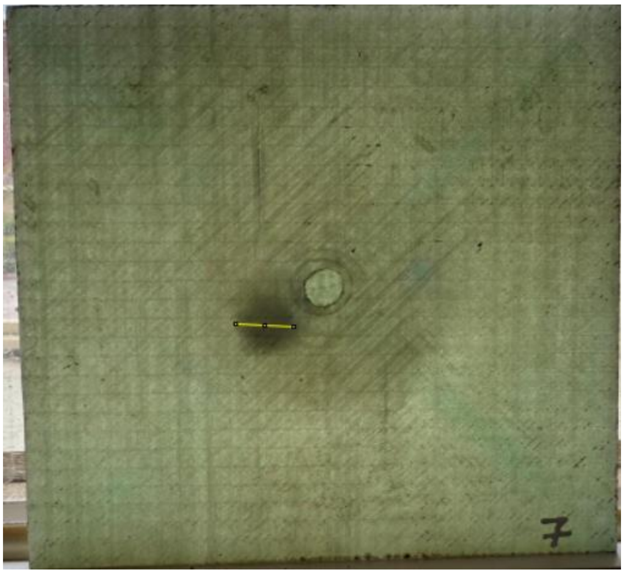

Specimen 7
Impact energy = 17.5 J
Impact location = 16 mm
Damage length= 14.5 mm

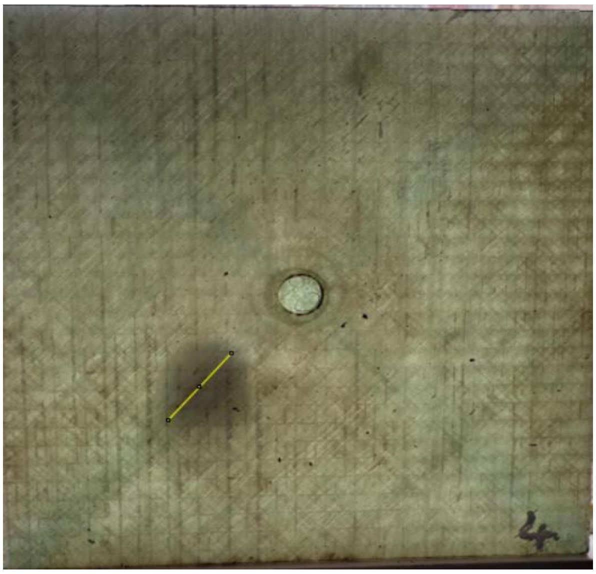

Specimen 4
Impact energy = 25 J
Impact location = 32 mm
Damage length= 23.5 mm

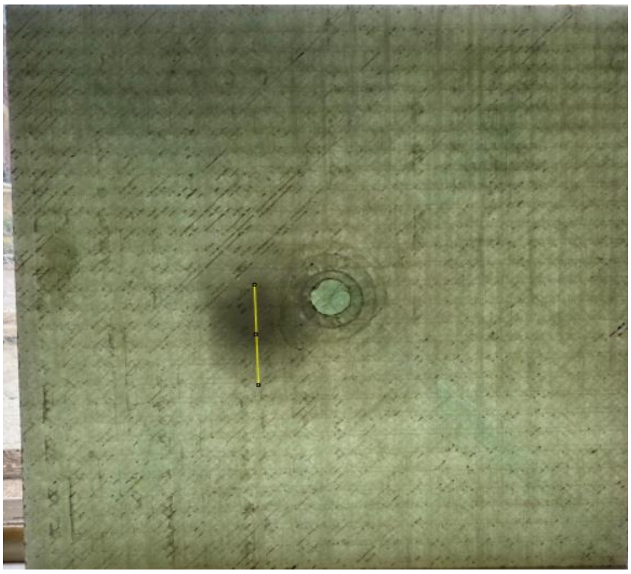

Specimen 10
Impact energy = 28 J
Impact location = 16 mm
Damage length= 26.4 mm

Figure 6. Specimen characteristics and damage dimensions

Table 3. Model Statistics metrics.

Model Summary Statistics	
Metric	Value
R-squared	0.9307
Adjusted R-squared	0.8812
F-value	18.8012
P-value	6.2584e-04

Table 4. Significance in ANOVA table

Term	Coefficient	P-value
Impact Energy	-0.9264	4.7202e-03
Impact Location	-1.6771	1.8515e-04
intersection	0.5902	0.16682

3.3 Experimental results

Following the statistical analysis and validation of the experimental data using R-squared and ANOVA, graphs were generated to explore and interpret the response trends. Firstly, the Factors vs. Biaxial Loading plot is shown in Figure 7., which illustrates the effect of each factor on biaxial loading. The blue curve represents the impact energy and biaxial loading, while the red curve represents the impact location and biaxial loading. Both curves show a negative correlation, meaning that the biaxial loading decreases as the energy increases and the location moves more toward the repair. A significant observation was conducted when comparing both factors on their effect on biaxial loading, and the impact locations show a steeper slope, indicating that the impact location has a more substantial influence on the biaxial than the impact energy. This suggests that if the impact occurs away from the repair centre and closer to the repair edge, the ability of the repaired composite to withstand the biaxial loading decreases.

Secondly, the combined effect was also studied and shown in a 2D contour shown in Figure 8. The colour gradient represents different biaxial loading values, the blue indicates the higher biaxial loading values, which means that the material could withstand more pressure before failure, and red colour indicates low values. After the contour was observed, the top left region (blue shades) occurred when the impact location was near the centre of the scarf repair, and the impact energy was low. The structure was more substantial and could withstand the pressure. However, in the bottom right (red shades), the combining effect of the impact location closer to the edge and the impact energy is high, and the biaxial loading decreased significantly. Finally, the most critical factor is the impact location, as it has a greater effect on biaxial loading.

The results obtained are like the experimental work done by Kumari et al [16,20] for unidirectional GFRP in his research; the impact location was also the more sensitive factor, and the edge of the repair was the critical location—additionally, the tensile test performed by Kumari et al. [16,20] confirmed that the specimen strength is weakened by higher impact energy. Similar results were obtained through the biaxial loading pressure implemented in this research.

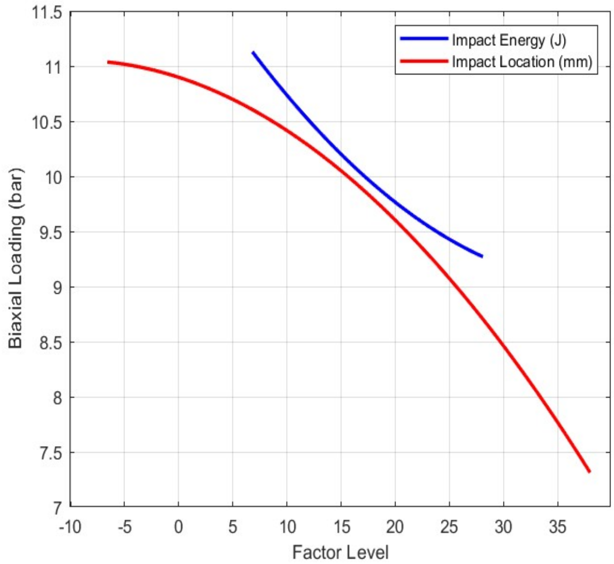

Figure 7. Factor level plot

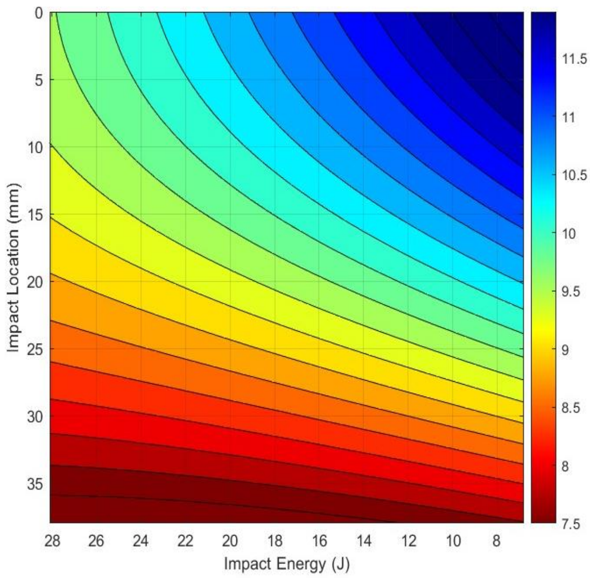

Figure 8. Contour plot

Conclusion

This study investigated the effect of the impact energy levels between 6 and 28 J. Different impact locations from the centre to the edge of the repair were chosen to cover a broad range of the expected impact scenarios affecting the performance of the repair. The specimens are exposed to pressure loading to generate a biaxial loading that the specimen can withstand. That test was chosen to get closer to the actual application, such as aeroplanes being exposed to pressure between the upper and lower surfaces, with lower pressure on top and higher pressure below, enabling flight. Finally, the data was taken from the central composite design model and studied to allow the understanding of the response tendencies after the factors' effects. The following can be concluded:

- The statistical model fits firmly since 93.07% of the variability in biaxial loading is explained.
- Impact energy and impact location are both significant factors. Both factors have a negative interaction on the response.
- The impact location was the more sensitive factor than the impact energy. This means it is essential to know the impact energy the repair was exposed to and its location.
- The repair edge and its nearby are the most critical impact locations compared to the central area of the repair.
- The contour analysis's combined effect of test factors shows an exponential drop in biaxial loading when high energy impacts occur at significant locations.

Reference

[1] Lee D S, Fahey D W, Forster P M, Newton P J, Wit R C N, Lim L L, Owen B and Sausen R 2009 Aviation and global climate change in the 21st century *Atmos Environ* **43** 3520–37

[2] Mashable A, Wolfe P, Ashok A, Dorbian C, He Q, Fan A, Lukachko S, Mozdzanowska A, Wollersheim C, Barrett S R H, Locke M and Waitz I A 2011 Assessing the environmental impacts of aircraft noise and emissions *Progress in Aerospace Sciences* **47** 15–52

[3] Parveez B, Kittur M I, Badruddin I A, Kamangar S, Hussien M and Umarfarooq M A 2022 Scientific Advancements in Composite Materials for Aircraft Applications: A Review *Polymers (Basel)* **14**

[4] Timmis A J, Hodzic A, Koh L, Bonner M, Soutis C, Schäfer A W and Dray L 2015 Environmental impact assessment of aviation emission reduction through the implementation of composite materials *International Journal of Life Cycle Assessment* **20** 233–43

[5] Abd El-baky M A 2018 Impact performance of hybrid laminated composites with statistical analysis *Iranian Polymer Journal (English Edition)* **27** 445–59

[6] Jefferson Andrew J, Arumugam V, Saravanakumar K, Dhakal H N and Santulli C 2015 Compression after impact strength of repaired GFRP composite laminates under repeated impact loading *Compos Struct* **133** 911–20

[7] Baker A, Gunnion A and Wang J 2015 On the certification of bonded repairs to primary composite aircraft components *Journal of Adhesion* **91** 4–38

[8] Orsatelli J-B, Paroissien E, Lachaud F, Schwartz S and Lachaud F 2023 Bonded flush repairs for aerospace composite structures Bonded flush re-pairs for aerospace composite structures: A review on modelling strategies and application to repairs optimization, reliability and durability. Composite Structures Bonded flush repairs for aerospace composite structures: a review on modelling strategies and application to repairs optimization, reliability and durability **304** 116338

[9] Budhe S, Banea M D and de Barros S 2018 Bonded repair of composite structures in aerospace application: a review on environmental issues *Applied Adhesion Science* **6**

[10] Bendemra H, Compston P and Crothers P J 2015 Optimisation study of tapered scarf and stepped-lap joints in composite repair patches *Compos Struct* **130** 1–8

[11] Odi R A and Friend C M 2002 A Comparative Study of Finite Element Models for the Bonded Repair of Composite Structures

[12] V Srinivasan D, Ravisankar Padma S and Idapalapati S 2022 Comparative study of composite scarf and strap joints for equivalent repair signature under uniaxial tension *Compos Part A Appl Sci Manuf* **158**

[13] Barbosa N G C, Campilho R D S G, Silva F J G D and Moreira R D F 2018 Comparison of different adhesively-bonded joint configurations for mechanical structures *Procedia Manufacturing* vol 17 (Elsevier B.V.) pp 721–8

[14] Cheng X, Zhao W, Liu S, Xu Y and Bao J 2014 Damage of scarf-repaired composite laminates subjected to low-velocity impacts *Steel and Composite Structures* vol 17 (Techno Press) pp 199–213

[15] Shufeng L, Xiaoquan C, Yunyan X, Jianwen B and Xin G 2015 Study on impact performances of scarf-repaired carbon fiber reinforced polymer laminates *Journal of Reinforced Plastics and Composites* **34** 60–71

[16] Kumari P, Alam A, Saahil, Wang J and Sankar S S 2020 Tensile after impact response on the scarf repaired glass fiber reinforced polymer samples - Experimental approach *Materials Today: Proceedings* vol 43 (Elsevier Ltd) pp 112–23

[17] Shankar S V and Idapalapati S 2023 Effect of Scarf Repair Geometry on the Impact Performance of Aerospace Composites *Polymers (Basel)* **15**

[18] DENG J, HUANG W and CHENG X 2024 Tensile Properties of Scarf-Repaired Composite Laminates with Bonding Defects *Applied Composite Materials*

[19] Cheng X, Du X, Zhang J, Zhang J, Guo X and Bao J 2018 Effects of stacking sequence and rotation angle of patch on low velocity impact performance of scarf repaired laminates *Compos B Eng* **133** 78–85

[20] Kumari P, Wang J and Saahil 2019 Tensile After Impact Test of Scarf-Repaired Composite Laminates *Arab J Sci Eng* **44** 7677–97

[21] Kumari P, Wang J and Saahil 2018 Residual tensile strength of the multi-impacted scarf-repaired glass fiber-reinforced polymer (GFRP) composites *Materials* **11**

[22] Anon [Wiley Series in Probability and Statistics] Raymond H. Myers, Douglas C. Montgomery, Christine M. Anderson-C - Response Surface Methodology_ Process and Product Optimization Using Designed Experiments (2009, Wi